# Fast and slow dynamics in the one-dimensional $\Phi^4$ lattice model: A molecular-dynamics study

S. Flach*

*Institut für Theoretische Physik, Technische Universität Dresden, Mommsenstrasse 13, D-8027 Dresden, Federal Republic of Germany*

J. Siewert

*Institut für Theoretische Festkörperphysik, Universität Karlsruhe, Engesserstrasse 7, Postfach 6980, D-7500 Karlsruhe 1, Federal Republic of Germany*

The separation of dynamics into slow and fast components for the one-dimensional $\Phi^4$ lattice model with a nearest-neighbor interaction is studied. We find two dynamic scaling laws for the displacement-displacement correlator in the strong-interaction case. The temperature window where scaling appears has a nonzero lower bound. There exist no analogies between the found scaling properties and structural relaxation processes in undercooled liquids near the liquid-glass transition. This fact seems to be due to the presence of static on-site double-well potentials. In the case of weak interaction only one dynamic scaling law seems to appear.

## I. INTRODUCTION

This work is concerned with the separation of dynamics into slow and fast components for a model of structural phase transitions. Over the past 10–20 years the dynamic and static properties of the scalar $\Phi^4$ lattice model were studied with various methods. A lot of work was devoted to the explanation of a central peak (CP) appearing in the dynamic structure factor in neutron-scattering studies of perovskite crystals near structural phase transitions (see Refs. 1 and 2 and references therein).

In Ref. 3 an intrinsic explanation for the CP appearance was derived by Aksenov, Bobeth, Plakida, and Schreiber (ABPS) using the $\Phi^4$ model. These authors started with the assumption that the CP appears due to the presence of precursor clusters of the low-symmetry phase in the high-symmetry phase (see also Ref. 1). The anomalous narrowing of the CP ABPS explained via a freezing of the cluster system at temperatures well above the phase transition, i.e., via a structural relaxation of a glasslike system. ABPS considered the equation of motion for the displacement-displacement correlation function $S_{lk}(t)$. Applying some approximation they derived closed self-consistent equations for $S_{lk}(t)$. These equations are called mode-coupling equations (MCE's) and were extensively studied by Götze[4] to describe freezing phenomena for undercooled liquids within mode-coupling theory (MCT) for normalized density-density correlators $\Phi_q(t)$. The most important feature of MCE's is the existence of a bifurcation point or a dynamic singularity. Near this singularity dynamic slowing down sets in and thus a separation of the dynamics (slow and fast) appears. The existence of the MCT singularity is not necessarily connected with divergences of static susceptibil-

ities in contrast to second-order phase transitions. The bifurcation point separates the control parameter space (e.g., the temperature axis) into a region of ergodic states $[\Phi_q(t \to \infty) = 0]$ and nonergodic states $[\Phi_q(t \to \infty) \neq 0]$. Thus, at $\omega = 0$ in the nonergodic region, a $\delta(\omega)$ peak at $\omega = 0$ in $\Phi_q(\omega)$ will appear.[4]

The present paper completes a number of studies[5–8] of the applicability of MCE to the $\Phi^4$ model as reported by ABPS. In Sec. II we introduce the model. Section III is devoted to the derivation of MCE's following ABPS (with some critical remarks) and to the main mathematical consequences following Götze.[4] In Sec. IV we present molecular-dynamics studies for one-dimensional $\Phi^4$ systems. We discuss our results in Sec. V. A summary is given in Sec. VI.

## II. MODEL

The model under consideration is the so-called $\Phi^4$ lattice model, which is often used to describe features of structural phase transitions.[1,9] Its Hamiltonian reads

$$H = \sum_{l=1}^{N} \left( \frac{1}{2} P_l^2 + V(X_l) \right) + \frac{1}{4} \sum_{l,k=1}^{N} C_{lk}(X_l - X_k)^2,$$

$$V(X) = -\frac{1}{2}X^2 + \frac{1}{4}X^4 . \tag{1}$$

Model (1) belongs to the universality class of the corresponding Ising model.[1] All variables and parameters in (1) are dimensionless. The corresponding transformation rules are given in Ref. 5. The index $l$ runs over all unit cells; $X_l$ and $P_l$ are the conjugated displacement and momentum of the $l$th particle, respectively. The coupling

constants $C_{lk} = C_{l+m,k+m} \geq 0$ determine the dimension of the system and the radius of interaction. The integrated interaction strength $C_0 = \sum_k C_{lk}$ is usually used to distinguish two different regimes of (1), namely, the displacive one (strong interaction $C_0 > 1$) from the order-disorder one (weak interaction $C_0 < 1$).[1,9] Earlier studies[10,11] suggested that in the displacive limit model (1) exhibits a soft phonon mode (being the reason for the phase transition), whereas in the order-disorder limit a separation of the motion into a fast (phonons) and a slow [hopping between the minima of the local potential $V(X)$] should take place.[1] Later, Bruce, Schneider, and Stoll showed by use of the universality class of (1) that also in the displacive limit the separation in the dynamics (slow and fast) sets in near the phase transition.[12,13] Thus the classical soft-mode picture of the phase transition breaks down even in the strong-interaction case (see also Ref. 14).

The mentioned separation of the dynamics naturally leads to a CP at zero frequency in the displacement-displacement correlation function $S_{lk}(\omega)$,

$$
\begin{aligned}
S_{lk}(t) &= \langle X_l(t) X_k \rangle \ , \quad S_{lk} = \langle X_l X_k \rangle \ , \\
S_{lk}(\omega) &= S_{lk}(z = \omega + i0) \ , \\
A(z) &= \mathrm{LT}[A(t)] = \frac{1}{i} \int_0^\infty dt \, e^{izt} A(t) \ .
\end{aligned}
\tag{2}
$$

Here $\langle \cdots \rangle$ denotes standard canonical average and $\mathrm{LT}[\cdots]$ means Laplace transformation. The exact influence of the separation of dynamics on the CP formation is very complicated. A lot of work was devoted to classify the dependence of the low-frequency part of $S_{lk}(\omega)$ on the temperature $T$ and interaction $C_{lk}$ both numerically and analytically.[13,15−23] In all only $S_{lk}(\omega)$ on a linear $\omega$ scale was studied. In Sec. IV we will show that a really powerful method is to look at the imaginary part of the susceptibility $\chi(\omega)$,

$$
\chi_{lk}''(\omega) = \tfrac{1}{2} \omega S_{lk}(\omega) \ ,
\tag{3}
$$

on a logarithmic frequency scale, as commonly done to study slow relaxations in glass dynamics.[4] It turns out that previous characterizations of the CP in $S_{lk}(\omega)$ can be replaced by a well-defined low-frequency analysis of $\chi_{lk}''(\omega)$.

Model (1) with a nearest-neighbor interaction (NNI) exhibits a phase transition at a finite temperature $T_c \neq 0$ for dimension $d \geq 2$,[24] whereas $T_c = 0$ for $d = 1$.[24] As we reported in Ref. 25 no indications of MCT predictions were found for $d = 2$ and a NNI. The same holds for the case $d \to \infty$ (mean-field case).[5,6,26] Here we will study the $d = 1$ case with a NNI.

### III. MODE-COUPLING APPROXIMATION

Using standard methods for the equation of motion of correlation functions (see Appendix A) one can write the following double fraction for the correlator $S_q(z)$ with $A_q = \sum_{\mathbf{k}} \exp[i\mathbf{q} \cdot (\mathbf{l} - \mathbf{k}) A_{lk}]$:[27]

$$
S_q(z) = \frac{T \chi_q^T}{z - \dfrac{1/\chi_q^T}{z - M_q(z)/T}} \ ,
\tag{4}
$$

$$
\chi_q^T = S_q(t = 0)/T \ .
$$

Here $T$ denotes the temperature of the system. The relaxation kernel $M_q(z)$ shall be expressed using two different methods, namely, the Tserkovnikov method[28,29] and the Mori method.[27] Both methods are projection operator methods. The Tserkovnikov method uses *frequency-dependent* projections:

$$
M_q(z) \equiv ((\ddot{X}_l | \ddot{X}_k))_q^{(2)}(z),
\tag{5}
$$

$$
\begin{aligned}
((A|B))_q^{(2)}(z) &= ((A|B))_q^{(1)}(z) - ((A|P))_q^{(1)}(z) \\
&\quad \times \frac{1}{((P|P))_q^{(1)}(z)} ((P|B))_q^{(1)}(z),
\end{aligned}
\tag{6}
$$

$$
\begin{aligned}
((A|B))_q(z) &= ((A|B))_q(z) - ((A|X))_q(z) \\
&\quad \times \frac{1}{((X|X))_q(z)} ((X|B))_q(z) \ ,
\end{aligned}
\tag{7}
$$

$$
((A|B))_q(t) = \langle A^\dagger(t) B(0) \rangle_q \ .
\tag{8}
$$

Within the Mori method the projection operators $\hat{P}$ and $\hat{Q}$ are *frequency independent*:

$$
M_q(t) = ((\hat{Q} \ddot{X}_q e^{i\hat{Q}\hat{L}\hat{Q}t} \hat{Q} \ddot{X}_q)),
\tag{9}
$$

$$
e^{i\hat{L}t} X_q = X_q(t) \ , \quad \dot{X}_q(t) = i\hat{L} X_q(t),
$$

$$
\hat{P} A = \sum_q (A|X_q) / (X_q|X_q) X_q + (A|P_q) / (P_q|P_q) P_q \ ,
\tag{10}
$$

$$
\hat{Q} = 1 - \hat{P} \ , \quad (A|B) = \langle A^\dagger B \rangle.
$$

Here we have to work with $q$-dependent sets of variables $\{X_q\}$ and $\{P_q\}$ to guarantee orthogonality $(X_q|X_{q'}) = (X_q|X_q) \delta_{q,q'}$. $\hat{L}$ denotes the Liouville operator. It is easy to see that $M_q(z)$ is invariant under the transformation $\ddot{X} \to \ddot{X} + a\dot{X} + bX$ for both representations. Note that if $S_q(t \to \infty) = L_q \neq 0$, then also $M_q(t \to \infty) \neq 0$, and both $S_q(z)$ and $M_q(z)$ have a pole at $z = 0 + i0$. But it is evident that even if a correlator $S_q(z)$ has a pole at zero frequency, all Laplace-transformed time derivatives of the correlator will be regular at zero frequencies (no pole):

$$
\lim_{z \to i0} z \mathrm{LT} \left[ \frac{d^n}{dt^n} S_q(t) \right] = 0 \ , \quad n \geq 1 \ .
\tag{11}
$$

Let us apply these sum rules (11) to the Tserkovnikov representation of the relaxation kernel [Eqs. (5)–(8)]. At first we have to calculate the pole of $M_q(z)$:

$$zM_q(z) = z((\ddot{X}|\ddot{X}))_q(z) - z((\ddot{X}|X))_q(z)\frac{z((X|\ddot{X}))_q(z)}{z((X|X))_q(z)} - \left[ ((\ddot{X}|\dot{X}))_q(z) - ((\ddot{X}|X))_q(z)\frac{z((X|\dot{X}))_q(z)}{z((X|X))_q(z)} \right]$$
$$\times \left[ \frac{1}{z}((\dot{X}|\dot{X}))_q(z) - ((\dot{X}|X))_q(z)\frac{((X|\dot{X}))_q(z)}{z((X|X))_q(z)} \right]^{-1}$$
$$\times \left[ ((\dot{X}|\ddot{X}))_q(z) - ((\dot{X}|X))_q(z)\frac{z((X|\ddot{X}))_q(z)}{z((X|X))_q(z)} \right] . \tag{12}$$

Performing the limit $z \to i0$ in (12) the first two terms on the RHS in line 1 vanish because of (11), the first terms in the angular brackets in lines 1 and 3 remain, and the *pole* of $M_q(z)$ comes from the angular bracket in line 2 in (12) (see also Appendix A). Hence decoupling methods (factorizations of higher-order correlation functions) have to take into account all angular brackets in (12). This was not done by ABPS; instead all angular brackets were neglected and a decoupling in the first two terms on the

RHS in line 1 led to the approximation[3]

$$M_{lk}(t) \approx 6[S_{lk}(t)]^3 . \tag{13}$$

On the other hand, one can use the same treatment of the Mori representation of the relaxation kernel as in the MCT.[4] There one has to project the force $\hat{Q}\ddot{X}_q$ onto the product of the initial variables $X_q$ in the lowest possible order using the new projection operator

$$\hat{P}_{\mathrm{MCT}}A = \sum_{q_1 < q_2 < \cdots < q_n} (A|X_{q_1}\cdots X_{q_n})/\langle |X|^2_{q_1}\cdots |X|^2_{q_n}\rangle X_{q_1}\cdots X_{q_n} . \tag{14}$$

Because of the symmetry of (1), the lowest possible order of $n$ is $n = 3$. After projection one has to decouple the correlators of the products into products of correlators, replacing the reduced time dependence by the full dynamics $\hat{Q}\hat{L}\hat{Q} \to \hat{L}$.[4] This mode-coupling approximation leads to an equation similar to (13):

$$M_q(t) \approx \sum_{q_1,q_2} V(q,q_1,q_2)S_{q_1}(t)S_{q_2}(t) \cdot S_{q-q_1-q_2}(t) . \tag{15}$$

If we allow all possible combinations $\{q_1,q_2,q_3\}$ of the triples $X_{q_1}X_{q_2}X_{q_3}$, as defined in (14), the calculation of the vertex $V(q,q_1,q_2)$ turns out to be complicated (see Appendix A) and cannot be given here in an analytical form. However remember that in our case we *know* that

$$\ddot{X}_l = -X_l^3 + (1 - C_0)X_l + \sum_{k \neq l} C_{lk}X_k . \tag{16}$$

Thus $\ddot{X}$ contains the product $X^3$ of the initial variable $X$ from the beginning. In this case it might be reasonable to proceed to the second step of the mode-coupling approach *immediately* and to decouple the products without additional projection (this is equivalent to a projection of $\ddot{X}_q$ onto $X_q^3 = 1/N^2 \sum_{q_1,q_2} X_{q_1}X_{q_2}X_{q-q_1-q_2}$). Then we simply derive

$$V(q,q_1,q_2) = \frac{6}{N^2} . \tag{17}$$

This result is identical with (13). But strictly speaking the calculation of $M_q(t)$ remains an open question.

Equations (4) and (15) or (4) and (13) are called mode-coupling equations in analogy to corresponding more general equations for the density-density correlator in liquids. Such types of equations have been extensively stud-

ied (see Ref. 4 and references therein) and successfully applied to describe the dynamics of undercooled liquids. These MCE's exhibit a dynamic slowing down due to the complicated feedback (15). The physical interpretation of one part of the slowing down for liquids is the cage effect. A particle rattles in a cage, formed by its neighbors. The cages relax very slowly near some bifurcation point due to the feedback. Passing the bifurcation, a tagged particle becomes localized in space. In other words, a complicated multiwell potential landscape originating from the interaction *forms at the bifurcation point*.[4] In Sec. V we will apply this physical interpretation to our results. But in the following let us assume the correctness of (15) for (1) and discuss in more detail the mathematical consequences as reviewed in Ref. 4.

Variations of the control parameter $T$ lead to variations of $S_q$. Then the MCE's describe generically a transition from ergodic states $S_q(t \to \infty) = 0$ to nonergodic states $S_q(t \to \infty) = L_q \neq 0$ at some temperature $T_c^{\mathrm{MCT}}$. This transition is an $A_2$ singularity following the notation of Ref. 4; i.e., for $T = T_c^{\mathrm{MCT}}$ the $L_q(T_c^{\mathrm{MCT}}) = L_q^c$ solutions are doubly degenerate. The whole $A_2$ scenario of MCT applies to the dynamics of $S_q(t)$, and thus two different dynamic scaling laws should appear for $T > T_c^{\mathrm{MCT}}$. Note that, at $T_c^{\mathrm{MCT}}$, $S_q$ is finite for all $q$; no static divergencies are necessary. The normalized correlator

$$\Phi_q(t) = S_q(t)/S_q \tag{18}$$

will exhibit an inflection point at $\Phi_q(t_{\mathrm{infl}}) \approx f_q^c = L_q^c/S_q(T_c^{\mathrm{MCT}})$. For $\delta\Phi_q(t) = \Phi_q(t) - f_q^c \ll 1$ and $\varepsilon = (T - T_c^{\mathrm{MCT}})/T_c^{\mathrm{MCT}}$ one obtains the $\beta$-scaling law[4]

$$\delta\Phi_q(t) = h_q\sqrt{\varepsilon}g(t/t_\varepsilon), \tag{19}$$

$$t_\varepsilon = \tau_0\varepsilon^{-1/2a} . \tag{20}$$

For $\Phi_q(t) < f_q^c$ one finds the $\alpha$-scaling law

$$\Phi_q(t) = F_q(t/\tau_\varepsilon), \tag{21}$$

$$\tau_\varepsilon = \tau_0 \varepsilon^{-1/2a - 1/2b}, \tag{22}$$

$$\frac{\Gamma^2(1-a)}{\Gamma(1-2a)} = \frac{\Gamma^2(1+b)}{\Gamma(1+2b)} = \lambda \quad . \tag{23}$$

$\Gamma(x)$ is the gamma function. The parameter $\lambda$ is model dependent. The master function $g(t)$ for the $\beta$-scaling law [Eqs. (19) and (20)] can be specified as

$$g(t) \sim t^{-a} \quad \text{for} \quad g(t) > 0 \ , \tag{24}$$

$$g(t) \sim -t^b \quad \text{for} \quad g(t) < 0 \ . \tag{25}$$

Note that in the case of a second-order phase transition only one dynamic scaling law of the type

$$\Phi_q(t) = \xi^A G(\xi^B q, \xi^C t) \tag{26}$$

should appear, where $\xi$ is the correlation length:[30]

$$\xi^2 = -\frac{1}{2} \frac{1}{S_{q=0}} \left[ \frac{d^2}{dq^2} S_q \right]_{q=0} \quad . \tag{27}$$

To be sure that the MCE's (4) and (15) lead to a transition at some $T_c^{\text{MCT}} > T_c$ for model (1) one has to calculate $S_q(T)$ and $V(q, q_1, q_2)$ [see (15)]. This seems to be impossible analytically. However, one can use the fact of the static critical behavior of (1) near $T_c$ and use the known critical exponents of the corresponding Ising model. It can be shown that near the phase transition of model (1) positive solutions $f_q \neq 0$ exist for $d = 1, 2, 3$ using (13) or (15) and (17) (Ref. 31 and Appendix B). Thus, increasing the temperature, one will find the nonergodic-ergodic transition at $T_c^{\text{MCT}} > T_c$ using (13), since for $T \to \infty$ only the $f_q = 0$ solution remains.

In the following we report on our studies of (1) by use of molecular dynamics. We try to find a temperature region above $T_c$ where dynamic slowing down appears. Then we test applicability of MCT with respect to the found slowing down.

## IV. MOLECULAR-DYNAMICS ANALYSIS

The results of Sec. IV are obtained by use of molecular dynamics for (1) with $d = 1$, $C_{lk} = C\delta_{l,k\pm1}$. We solve the classical Newton equations of motion using the Verlet algorithm[32] with periodic boundary conditions. The total energy of the system was conserved (microcanonical simulation). The time step was $h = 0.005$. The system size was $N = 8000$. In all cases the size of the system was of the order of $100\xi$ or larger. Comparing our results with runs for $N = 4000$ and different time steps we can definitely exclude any $h$ and $N$ dependence of our results. The energy was conserved within 0.001% during one run. The total simulation time of one run was $t_0 = 10^4 - 10^7$. To make sure we calculate the correct properties we performed two independent runs with random initial conditions at each temperature. Then we mapped both solutions onto each other to see that our results are reproducible.

The following quantities were calculated during one run: the temperature $T = \frac{1}{N} \sum_l \frac{1}{t_0} \int_0^{t_0} \dot{X}_l^2(t) dt$, the mean-square displacements

$$S_{lk} = \langle X_l X_k \rangle = \frac{1}{N} \sum_m \frac{1}{t_0} \int_0^{t_0} X_m(t) X_{m+k-l}(t) dt,$$

the mean cluster length $\langle l \rangle$ (mean length of chain parts with equal sign of particle displacements), the mean constant sign time $\langle \tau \rangle$ (mean time of constant sign of one particle displacement), distribution functions of cluster lengths and mean constant sign times, and the local time-dependent correlator

$$S_{ll}(t) = \frac{1}{N} \sum_l \frac{1}{t_0} \int_0^{t_0} X_l(t' + t) X_l(t') dt' \ . \tag{28}$$

The Laplace transformation of $S_{ll}(t)$ we performed using the Filon algorithm.[33]

### A. Strong-interaction case (displacive limit)

In this subsection we report on our results for $C = 4$. This value corresponds to the strong interaction case of (1), and following Aubry[15] it is possible to introduce a reduced temperature $T_r \sim T/\sqrt{C}$. Thus changing the interaction strength is equivalent to rescaling the temperature.

#### 1. Static properties

As we reported in Ref. 7 the inverse mean cluster length $\langle l \rangle$ as a function of temperature tends to zero at $T \approx 0.35$. At this temperature the $\langle l \rangle(T)$ dependence changes essentially. This may be considered as a crossover temperature $T^*$ or a "suppressed phase transition" temperature $T^*$. From our $S_{lk}$ data we obtained the spatial Fourier-transformed structure factor $S_q$ (Fig. 1):

$$S_q = \sum_k e^{iq(l-k)} S_{lk} \ . \tag{29}$$

Fitting the $q$ dependence for small $q$ we extracted the correlation length defined in (27), shown in the insert in Fig. 1. It turns out that $\xi$ is equal to $\langle l \rangle$ within 10% of error. Thus the interpretation of $T^*$ in terms of a suppressed phase transition seems to be reasonable. The fact that at $T^*$ some thermodynamic properties of (1) exhibit unusual properties is confirmed by plotting the inverse local static susceptibility

$$1/\chi_{ll} = T/S_{ll} \tag{30}$$

in Fig. 2. Clearly we see a bend at $T^* = 0.35$. It shall be noted here that Aubry found a maximum in the specific heat at $T \approx 0.4\sqrt{C/4} = 0.4$.[15] This maximum seems to correspond with our crossover temperature $T^*$.

Finally in Fig. 3 a semilogarithmic plot of the cluster length distribution function $P_{\langle l \rangle}(l)$ for different temperatures is shown. It is seen that $P_{\langle l \rangle}(l) \sim \exp(-\alpha l)$ in a large-$l$ region. Assuming random (uncorrelated) positions of cluster boundaries one easily derives

$$P_{\langle l \rangle}(l) \approx \frac{1}{\langle l \rangle} \left( 2 - \frac{1}{\langle l \rangle} \right) e^{-2l/\langle l \rangle} \ . \tag{31}$$
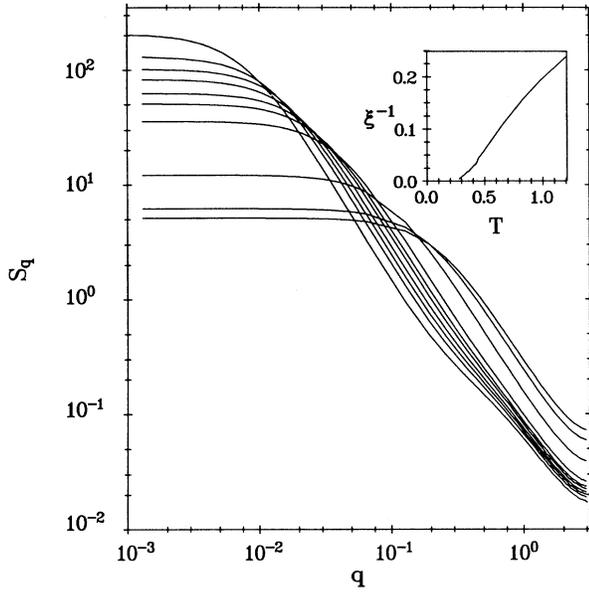
FIG. 1.  $S_q$ vs wave number $q$ for $C = 4$ and temperatures $T$ =0.28, 0.305, 0.331, 0.346, 0.387, 0.404, 0.445, 0.653, 0.986, and 1.2. Higher temperatures correspond to lower values of $S_q$ for $q \to 0$. Inset: Inverse mean correlation length $\xi^{-1}$ vs $T$ for $C = 4$.

Decreasing the temperature leads to increasing $\langle l \rangle$ and thus to decreasing $\alpha$. Although the assumption of un-correlated cluster boundary positions does not give the correct value of $\alpha$ (50% error), the temperature depen-dence of $\alpha$ can be qualitatively explained.
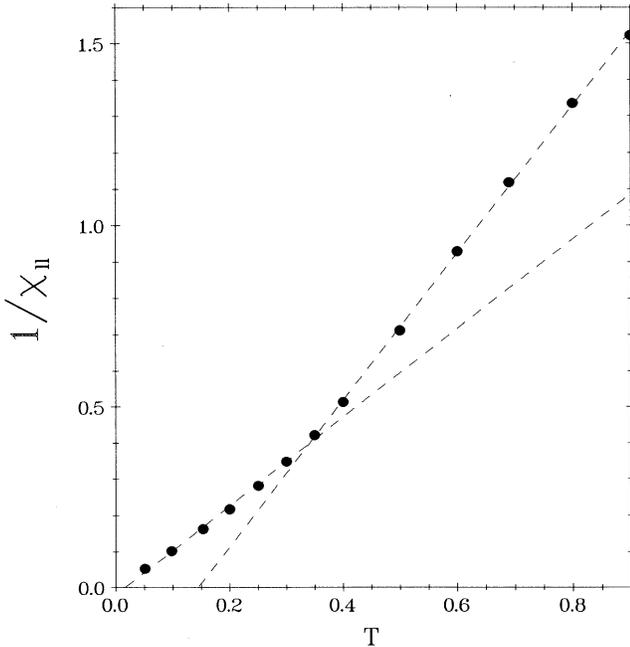


FIG. 2.  Inverse static local susceptibility $1/\chi_{ll}$ vs temper-ature for $C = 4$ (solid circles). The dashed lines are linear fits of $1/\chi_{ll}[T]$ for $T < 0.35$ and $T > 0.35$, respectively. A bend at $T = 0.35$ is seen.
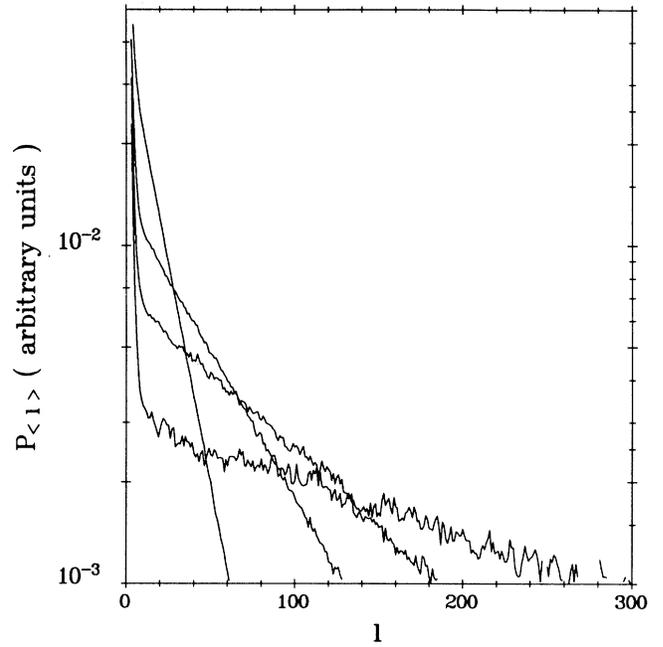


FIG. 3.  Cluster length distribution function $P_{\langle l \rangle}$ vs cluster length $l$ for $C = 4$ and $T = 0.3, 0.35, 0.4$, and 0.59. Higher temperatures correspond to larger slopes of $\log_{10}[P_{\langle l \rangle}]$ vs $l$ for large $l$.

## 2. Dynamic properties

As we reported in Ref. 7 the inverse mean constant sign time $\langle \tau \rangle$ as a function of temperature tends to zero at $T^*$. In Ref. 8 we started to analyze the frequency dependence of the imaginary part of the normalized susceptibility

$$\varepsilon_{ll}''(\omega) = \chi_{ll}''(\omega)/S_{ll} \; . \tag{32}$$

$\varepsilon_{ll}''(\omega)$ exhibits a high-frequency two-peak excitation spec-trum, which can be explained by motions of particles in one cluster.[8] In the low-frequency region $\omega < 1$ we found a minimum of $\varepsilon_{ll}''(\omega)$ at $\omega = \omega_{\beta'}(T)$ and at lower fre-quencies a maximum at $\omega = \omega_{\alpha'}(T)$, $\omega_{\alpha'}(T) < \omega_{\beta'}(T)$ (Fig. 4). The value $\omega_{\beta'}$ is nearly temperature indepen-dent in contrast to MCT [Eq. (20)]. The height of the minimum $\varepsilon''(\omega_{\beta'})$ decreases with decreasing temperature, but we found no $\varepsilon''^2(\omega_{\beta'}) \sim (T - T_c^{\mathrm{MCT}})$ dependence in contrast to (19).[8] Surprisingly we find a scaling law around the $\beta'$ minimum as shown for the scaled func-tion $\varepsilon_{ll,\beta'}''(\hat{\omega}) = \varepsilon_{ll}''(\hat{\omega}\omega_{\beta'})/\varepsilon_{ll}''(\omega_{\beta'})$, $\hat{\omega} = \omega/\omega_{\beta'}$, in a log-log-plot in Fig. 5. For $T = 0.33, 0.346, 0.364$ we find a master function on the low-frequency side of the $\beta'$ min-imum over one decade in frequency. The master func-tion can be fitted by a power law $\hat{\omega}^{-b}$ with $b \approx 1$ [cf. (25)]. This value leads to $\lambda = 0.5$ [Eq. (23)]. It shall be noted here that $1 > \lambda \geq 1/2$.[4] For lower temperatures $T = 0.3, 0.28$ we see a possible breaking of the scaling behavior on the low-frequency side of the $\beta'$ minimum. Now we stretch the $\omega$ scale on the high-frequency side of the $\beta'$ minimum (Fig. 6). We again see a scaling behav-ior for $T = 0.33, 0.346, 0.364$. But the master function
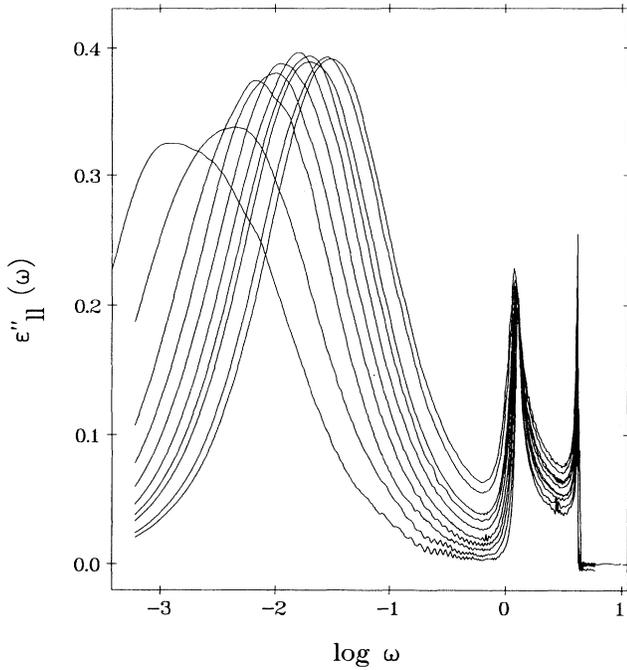
FIG. 4.   $\varepsilon_{ll}''$ vs $\log_{10}(\omega)$ for $C = 4$. $T = 0.28$, 0.305, 0.331, 0.346, 0.364, 0.379, 0.397, 0.404, 0.432, and 0.445.  Higher temperatures correspond to larger values of $\varepsilon_{ll}''$ in the $\beta'$ minimum.
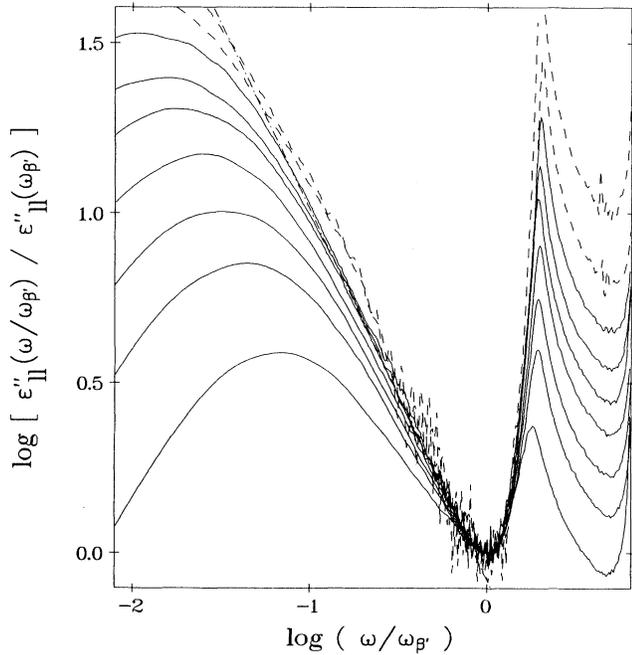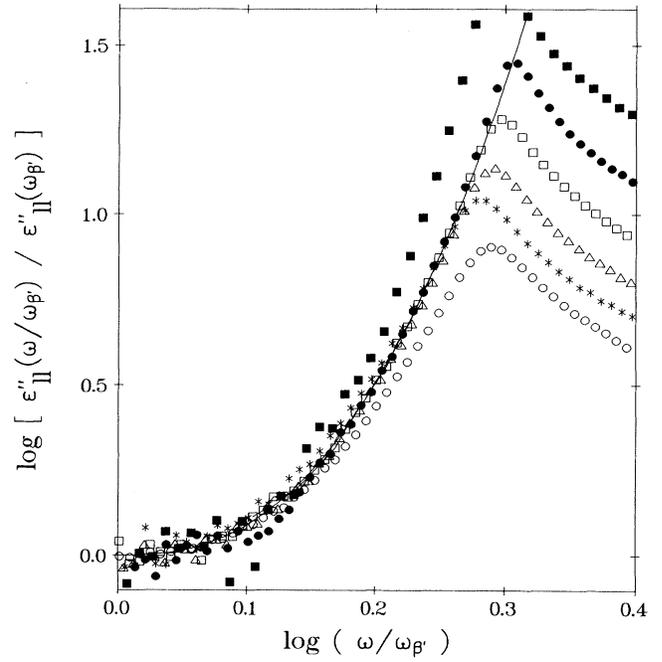


FIG. 6.   Same as Fig. 5 but on a stretched frequency scale. Only the right-hand side of the $\beta'$ minimum is seen.  Solid squares, $T = 0.28$; solid circles, $T = 0.305$; squares, $T = 0.331$; triangles, $T = 0.346$; stars, $T = 0.364$; circles, $T = 0.379$.  Clearly a master function (solid line) is observed for $T > 0.3$.



FIG. 5.   Scaled $\varepsilon_{ll}''/\varepsilon_{ll}''(\omega_{\beta'})$ vs scaled frequency $\omega/\omega_{\beta'}$ for the $\beta'$ minimum in a $\log_{10}$-$\log_{10}$ plot for $C = 4$.  Solid lines: $T = 0.331$, 0.346, 0.364, 0.379, 0.404, 0.432, and 0.487.  Dashed lines: $T = 0.28$ and 0.305.  Higher temperatures correspond to lower values of the scaled function outside the $\beta'$ minimum. The dashed-dotted line is a power fit $\chi_{ll}'' \sim \omega^{-b}$ with $b \approx 1$. The fluctuations of the dashed lines near the $\beta'$ minimum are numerical uncertainties.
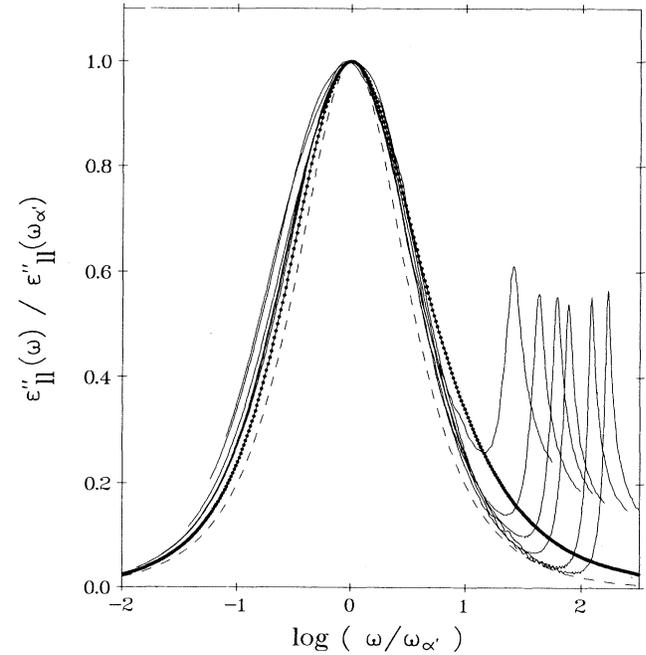


FIG. 7.   Scaled $\varepsilon_{ll}''/\varepsilon_{ll}''(\omega_{\alpha'})$ vs $\log_{10}$ of the scaled frequency $\omega/\omega_{\alpha'}$ for $C = 4$.  Solid lines: $T = 0.331$, 0.346, 0.379, 0.404, 0.432, and 0.487.  Higher temperatures correspond to larger values of the height of the $\beta'$ minimum.  Kohlrausch fit (see text), solid circles, and Debye fit (see text), dashed line.
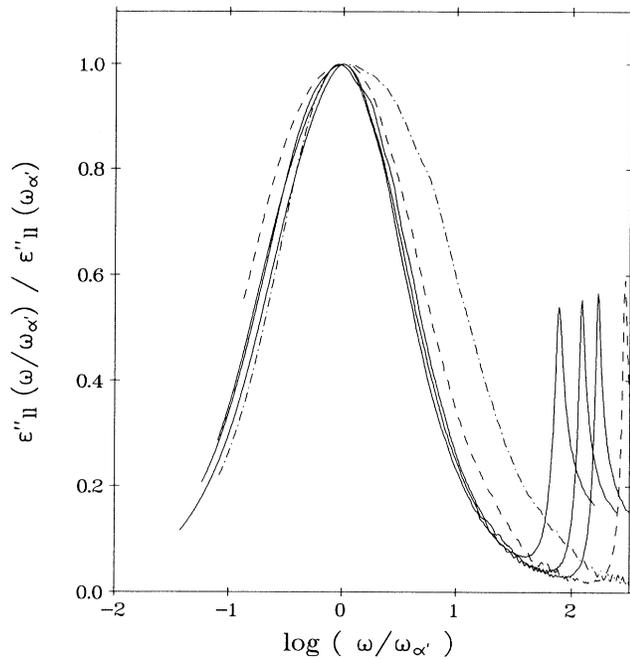
FIG. 8.    Same as in Fig. 7 but with solid lines, $T =$ 0.331, 0.346, and 0.379; dashed line, $T = 0.305$; dashed-dotted line, $T = 0.28$.
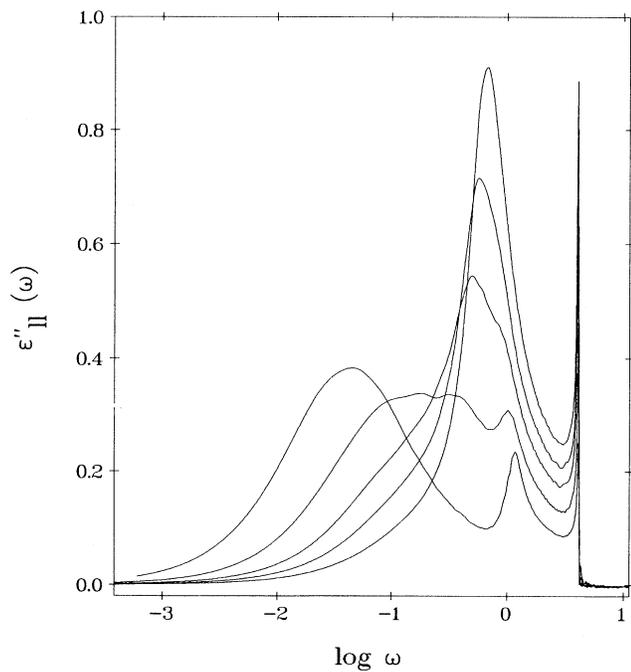


FIG. 9.    Same as in Fig. 4 but with $T = 0.487$, 0.653, 0.83, 0.986, and 1.2. Higher temperatures correspond to lower values of the low-frequency part $\omega < 10^{-2}$.



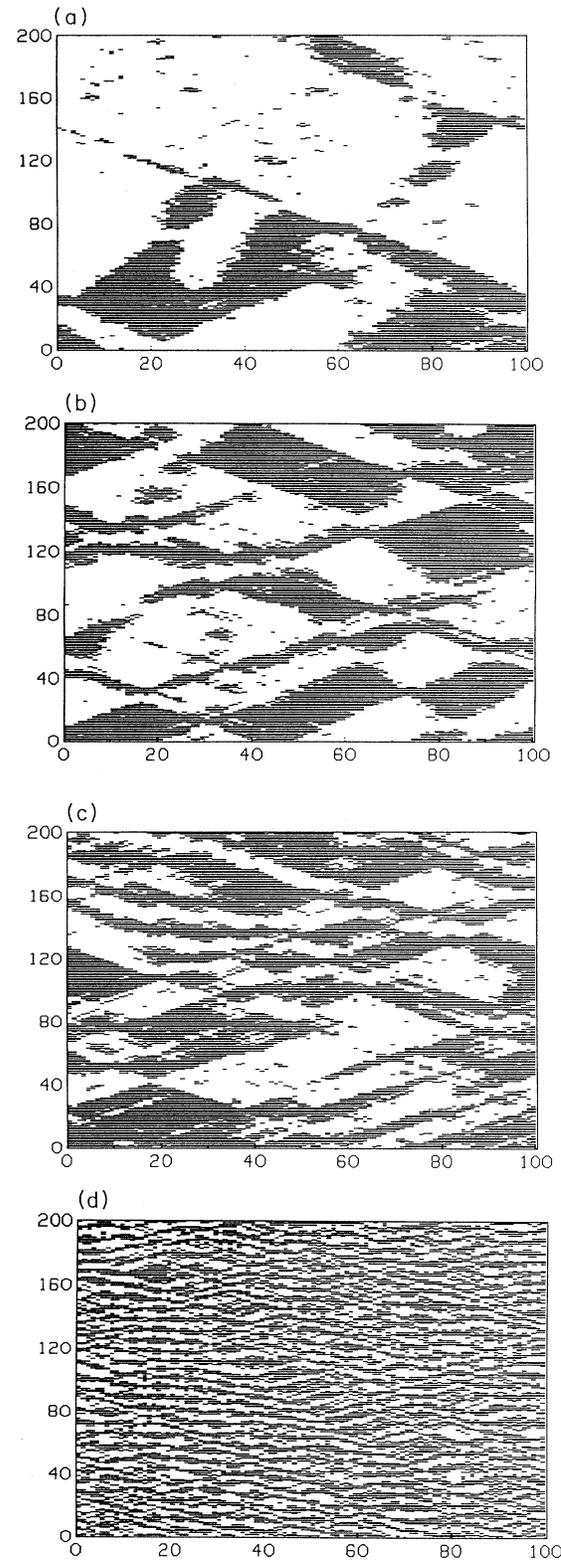FIG. 10.    Hypsometric plots for $C = 4$.    Abscissa (0,...,100), particle number $l$ within the chain; ordinate (0,...,200), $t/0.6$.    Dark areas, positive sign of $X_l(t)$; white areas, negative sign of $X_l(t)$.  (a) $T = 0.5$, (b) $T = 0.7$, (c) $T = 0.9$, and (d) $T = 10$.

cannot be fitted by a power law in contradiction to (24). Again the curve for the lowest temperature $T = 0.28$ falls out of the scaling region. Thus we find a scaling region for the $\beta'$ minimum $0.3 < T \leq 0.364$. Note that the crossover temperature $T^*$ introduced by the static properties analysis lies within this scaling window.

The $\alpha'$ maximum shifts to lower frequencies with decreasing temperature. Its height does not vary significantly for $T > 0.3$. But for $T \leq 0.3$ there appears a jump—$\varepsilon''(\omega_{\alpha'})$ decreases rapidly (Fig. 4). To analyze the scaling properties let us first look at temperatures $T > 0.3$. In Fig. 7 we see that a scaling law is valid for the scaled function $\varepsilon''_{ll,\alpha'}(\tilde{\omega}) = \varepsilon''_{ll}(\tilde{\omega}\omega_{\alpha'})/\varepsilon''_{ll}(\omega_{\alpha'})$, $\tilde{\omega} = \omega/\omega_{\alpha'}$. The master function can be partially fitted by a Kohlrausch law

$$S_{ll}(t) \sim e^{-[t/\tau(T)]^\beta} \quad . \tag{33}$$

The Kohlrausch exponent $\beta \approx 0.8 \pm 0.02$ (see solid circles in Fig. 7). Especially the high-frequency side of the $\alpha'$ master function cannot be described by (33). We also observe slight differences on the low-frequency side of the master function. A fit with a Debye law $S_{ll}(t) \sim \exp[-t/\tau(T)]$ cannot account for the $\alpha'$ peak (see dashed line in Fig. 7). Thus we observe a slightly stretched $\alpha'$ relaxation. In Fig. 8 we show the breaking of the $\alpha'$ scaling law for $T = 0.3, 0.28$. Clearly an additional stretching of the $\alpha'$ maximum appears. It follows for both $\alpha'$ and $\beta'$ analysis that the observed dynamic scaling region is limited in temperature to $T > 0.3$. Using the reduced temperature $T_r$ we find for the lower limit $T > 0.15\sqrt{C}$. The found scaling properties therefore cannot be attributed to the phase transition of (1)
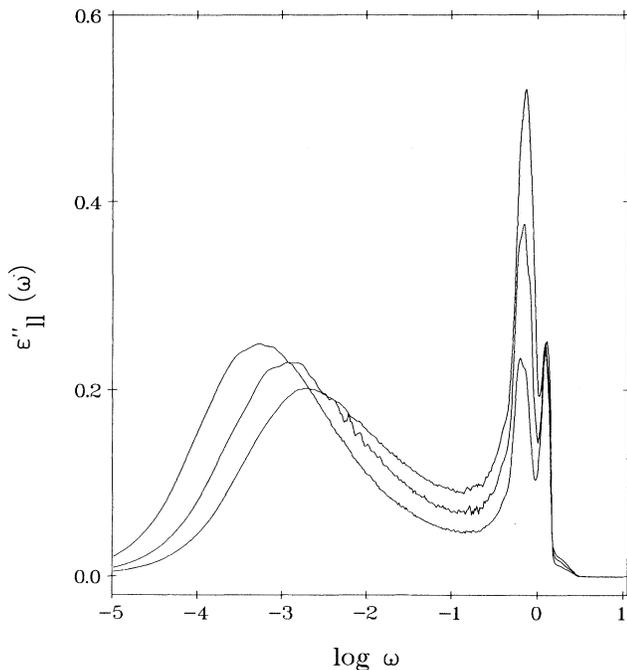


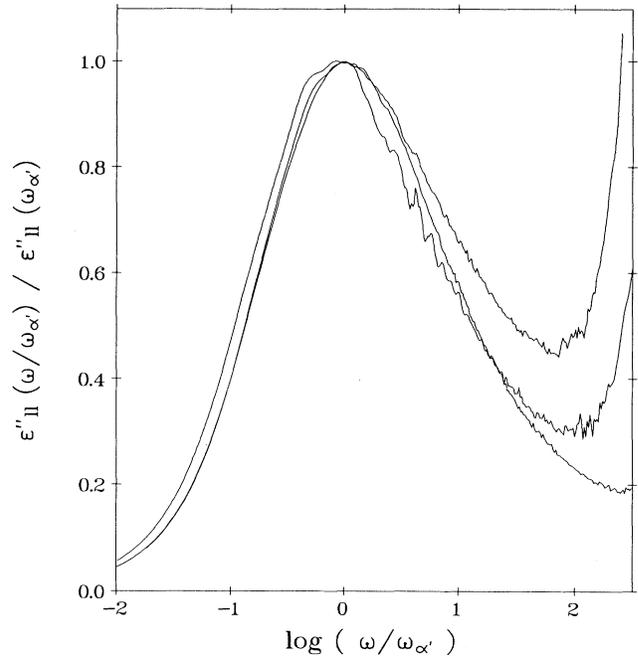FIG. 12. Same as in Fig. 7 but with $C = 0.1$ and $T = 0.106$, 0.126, and 0.151. Higher temperatures correspond to larger values of the height of the $\beta'$ minimum.



FIG. 11. Same as in Fig. 4 but with $C = 0.1$ and $T = 0.106$, 0.126, and 0.151. Higher temperatures correspond to larger values of the $\beta'$ minimum.
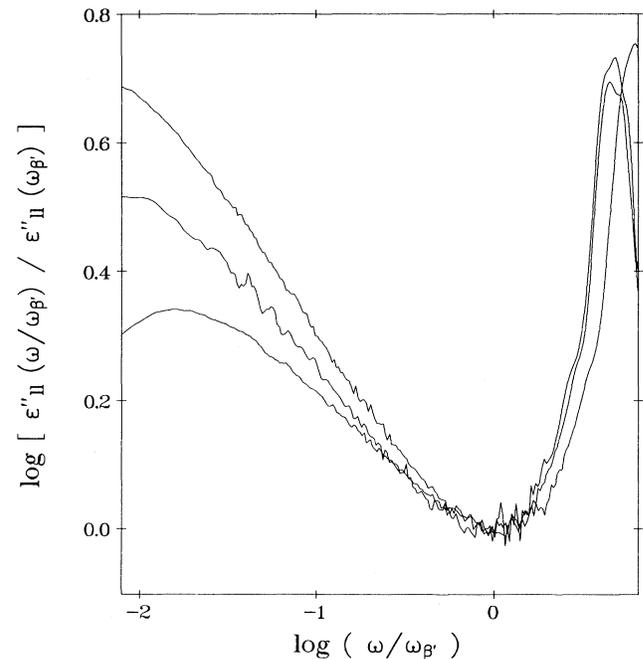


FIG. 13. Same as in Fig. 5 but with $C = 0.1$ and $T = 0.106$, 0.126, and 0.151. Higher temperatures correspond to lower values of the scaled function outside the $\beta'$ minimum.

at $T = 0$.

In Fig. 9 the $\varepsilon_{ll}''(\omega)$ data for higher temperatures $T <$ 1.2 are plotted. The $\alpha'$ maximum shifts to higher frequencies and at $T \approx 0.9$ ($T \approx 0.45\sqrt{C}$) coalesces with the lower-frequency peak of the high-frequency spectrum.

Finally we show in Fig. 10 so-called hypsometric plots of the particle positions for different temperatures. In these plots (particle number versus time on the axes) a particle is marked by a dot if its sign is positive and is not marked if the sign is negative. These plots are used to detect solitary excitations.[20] Clearly we see propagating cluster walls (kinks) with velocities $v_k = 1, ..., 2$ for $T \leq$ 0.9.

## B. Weak-interaction case (order-disorder limit)

In this subsection we will discuss the dynamic properties of (1) for $C = 0.1$. As we showed in Ref. 7 at $T = 0.1$ one can expect a crossover in analogy to $C = 4$, however only due to an increasing of the mean constant sign time $\langle \tau \rangle$ (see Fig. 5 in Ref. 7). The correlation length does not exhibit unusual behavior at this temperature ($\xi < 5$ for $T > 0.1$). Again we observe a high-frequency two-peak spectrum in $\varepsilon_{ll}''(\omega)$ with peak positions at $\omega \approx 0.66$ and $\omega \approx 1.3$ (Fig. 11). This part of the spectrum can be qualitatively attributed to the spectrum of a single particle moving in a double-well potential.[34] In the low-frequency region of $\varepsilon_{ll}''(\omega)$ again a $\beta'$ minimum and a $\alpha'$ peak are
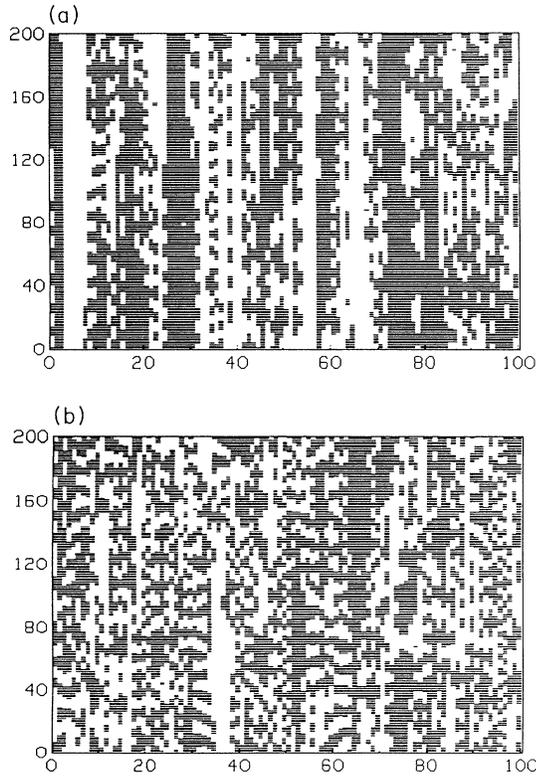


FIG. 14. Hypsometric plots for $C = 0.1$ (cf. Fig. 10). (a) $T = 0.2$ and (b) $T = 0.5$.

observed. As in the strong-interaction case the $\alpha'$ peak shifts to lower frequencies with lowering the temperature, whereas the $\beta'$ minimum does not shift. A scaling analysis shows that there is an indication of an $\alpha'$ scaling for $T \leq 0.125$ (Fig. 12). However, no $\beta'$ scaling is observed (Fig. 13). Thus only one dynamic scaling law ($\alpha'$ peak) seems to be present. In Figs. 14(a) and 14(b) hypsometric plots for $T = 0.2$ and 0.5, respectively, are shown. No propagating kinks can be detected.

## V. DISCUSSION

Let us first interpret our results in terms of MCT. The nonapplicability of (15) in the strong-interaction case follows from the (i) nonshifting of the $\beta'$ minimum of $\varepsilon''(\omega)$ with temperature, (ii) nonlinear $\varepsilon''^2(\omega_{\beta'})[T]$ dependence, and (iii) nonexistence of a power law on the high-frequency side of the $\beta'$ master function.

In terms of MCT we can say that we are far away from any dynamic singularity as described by that theory. All arguments listed above are concerned with the $\beta'$ minimum. The corresponding time window for $S_{ll}(t)$ is the decay onto a plateau (see Fig. 1 in Ref. 8). If $\omega_{\beta'}$ does not shift with temperature, the time $S_{ll}(t)$ needs to decay onto the plateau also does not change. This time is about three to four periods of the short-time oscillations,[8] and thus this decay process (onto the plateau) takes place on microscopic time scales. In contrast the corresponding decay within MCT (and experiments confirming MCT for liquids) takes place on mesoscopic time scales, five to ten decades larger than the microscopic time scales. What is the reason for the short-time scale of the $\beta'$ relaxation in our system? For low temperatures we have a dilute gas of propagating kinks in the strong-interaction case. The mean velocity of these kinks does not vary essentially with temperature.[16] The whole short-time dynamics then comes from the dynamics in one cluster. In this cluster all particles are displaced and oscillate around the mean nonzero position $\bar{X}$. Then the correlator $S_{ll}(t)$ will decay onto $\bar{X}^2$ for times large compared with the oscillation time. The presence of propagating kinks finally leads to some relaxation of the correlator to zero. Thus the $\beta'$ relaxation onto the plateau comes from the time average over some short-time oscillations in a cluster. The $\alpha'$ relaxation from the plateau comes from the presence of propagating kinks. Since by lowering the temperature the density of the kink gas is lowered (the correlation length increases), the $\alpha'$ relaxation takes place at larger times with decreasing temperature. The presence of clusters originates in the double-well on-site potential in (1). Thus the $\beta'$ relaxation comes from the trapping of a particle in one of the two minima of $V(X)$ due to the appearance of kinks. In other words, the particle becomes localized in the static on-site double-well potential $V(X)$. This "cage" does not relax in time in contrast to MCT. No stretching of the $\beta'$ process then occurs. In Ref. 31 the presented data for the static structure factor $S_q$ (Fig. 1) were used as inputs in (B1) to calculate $f_q$. There $0.98 < T_c^{MCT} < 1.2$ was found. Clearly no low-frequency anomalies in $\varepsilon''(\omega)$ are observed in this temperature region (Fig. 9).

In the weak-interaction case the reason for the separation of dynamics of $S_{ll}(t)$ into slow and fast components is the existence of nearly conserved variables, namely, effective one-particle energies. For $C = 0$ these nearly conserved variables become exact integrals of motion.[6] Thus the decay onto the plateau in $S_{ll}(t)$ corresponds to the dynamics of an isolated particle in the *static* on-site double-well potential $V(X)$. Again the particle becomes localized in one of the two minima, and this "cage" does not relax in time. By the same way one can explain the nonstretching of the decay onto the plateau as reported by Kob and Schilling[26] for finite systems (1) with infinite-range interaction $C_{lk} = C_0/N$. We can summarize that the on-site double-well potentials in (1) play the dominant role in the formation of a "cage" for one particle. This seems to be the reason for nonapplicability of MCT.

However, Prigodin[35] has shown that (1) with one minimum on-site potentials $V(X) = X^2 + \gamma X^4$ and *random* interaction $C_{lk} = d_{lk}/N$, $d_{lk}$ being randomly distributed around zero, can lead to applicability of MCT. The appearance of the stretching of the $\beta$ relaxation has to be attributed to the randomness of interaction. The "cage" one particle "feels" probably originates from the interaction with all other particles, and thus this "cage" can relax in time.

So far we discussed our results in terms of MCT. However, we can also make a conclusion about the applicability of the more general assumption of ABPS viewing the appearance of the narrow CP as due to a structural relaxation of a glasslike system (of clusters). As recent light-scattering experiments near the liquid-glass transition[36] show, the main features of systems exhibiting a dynamic liquid-glass transition indeed are (i) the power law $\varepsilon''(\omega) \sim \omega^a$, $a < 0.4$, on the high-frequency side of the $\beta$ minimum [being the reason for the enhancement of the values of $\varepsilon''(\omega)$ in the $\beta$ relaxation regime well above the white-noise behavior] and (ii) the von Schweidler relaxation $\varepsilon''(\omega) \sim \omega^{-b}$, $b < 1$, on the low-frequency side of the $\beta$ minimum. Both features are not found for our system. Thus the ABPS assumption seems to fail also from this more general point of view in the cases studied above.

From the discussion above it follows that the $\alpha'$ peak in $\varepsilon''_{ll}(\omega)$ can be attributed to the presence of propagating kinks in the case of strong interaction. From the coalescence of the $\alpha'$ peak with the high-frequency part at $T \approx 0.9$ we find that kinks disappear at higher temperatures. This conclusion agrees with hypsometric plot studies of Kerr and Bishop.[22] The existence of the corresponding nonlinear solutions was shown by Krumhansl and Schrieffer[37] and Aubry[16] for the continuum limit of (1). The dynamic properties were usually studied for the frequency-dependent correlator $S_q(\omega)$. In Fig. 15 we show the $S_{ll}(\omega)/S_{ll}(\omega = 0)$ curves for $C = 4$. From these curves we can only find the presence of a central peak at zero frequency, which width decreases with decreasing temperature. Clearly a much better analysis can be done studying the susceptibilities (Fig. 4). The temperature dependence of the width of the central peak can be attributed to the shifting of the $\alpha'$ maximum. The discussed dynamic scaling in the susceptibility would not be
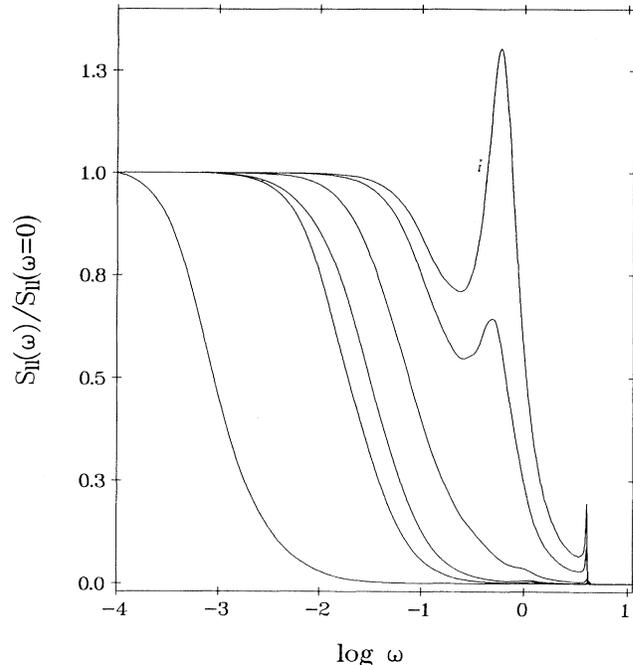


FIG. 15.  $S_{ll}(\omega)/S_{ll}(\omega = 0)$ vs $\log_{10}(\omega)$ for $C = 4$ and $T = 0.28$, 0.432, 0.487, 0.653, 0.986 and 1.2 (from left to right).

possible in $S_{ll}(\omega)$, and even the clear distinguishing between different contributions to high-frequency and low-frequency parts of the spectra is possible only for $\varepsilon''(\omega)$.

The appearance of the $\alpha'$ peak in the case of weak interaction probably can be attributed to a relaxation of nearly conserved variables. It is surprising that although the correlation length was short in the temperature window under study, indications for a dynamic scaling law can be found. Again the phase transition at $T = 0$ seems not to be the reason for its appearance.

So far we have only discussed the low-frequency properties of $S_{ll}(\omega)$. But it is interesting to note that there are features of the high-frequency properties of $S_{ll}(\omega)$, being connected with the results listed above. First let us mention that for $C = 4$ at $T = 0.9$ the mean-square displacements $S_{ll}(t = 0)[T] = S_{ll}[T] = \langle X_l^2 \rangle[T]$ have a minimum.[7] This property seems to correlate with the creation of kinks as suggested from the temperature dependence of the $\alpha'$ peak. In an isolated double-well potential $\langle X^2 \rangle$ also exhibits a minimum at a temperature comparable with the height of the energy barrier of the potential.[5] Thus we might conclude that for $T > 0.9$ for $C = 4$ the particle overcomes some potential barrier. But then one expects that at the same temperature the particle position and thus the correlator $S_{ll}(t)$ change their sign within the first period of oscillation, since in the opposite case the particle cannot overcome the barrier, it is "localized," and the sign of its time-dependent position does not change during the first oscillation. Indeed in Fig. 16 it is seen that around $T = 0.9$ the change of sign of $S_{ll}(t)$ during the first oscillation period takes
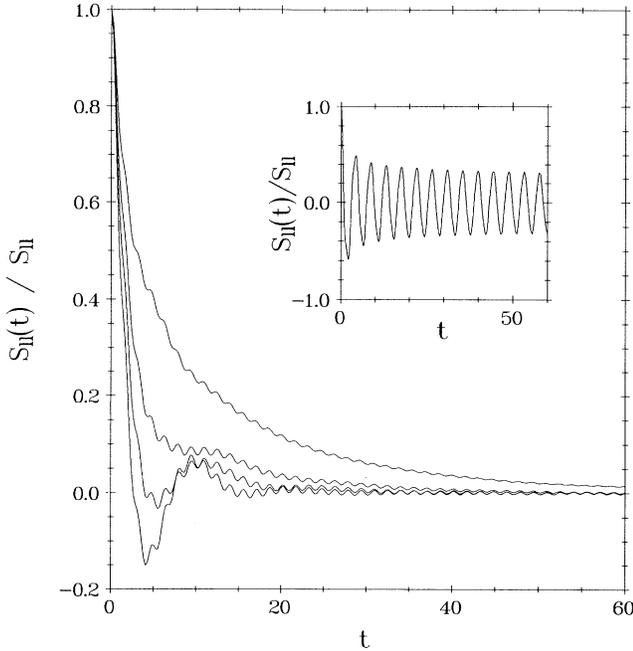
FIG. 16.   $S_{ll}(t)/S_{ll}(t = 0)$ vs time $t$ for $C = 4$ and $T = 0.653, 0.83, 0.986$, and $1.2$ (from top to bottom). Inset: Same for a harmonic chain (see text) with $C = 4$, $T = 1$.

place. From Fig. 16 also follows that in the temperature range $0.65 \leq T \leq 1$ $S_{ll}(t)$ is nearly temperature independent for times $t \geq 30$ and oscillates with a frequency $\omega_0 \approx 4.24$. This value corresponds to the position of the *high*-frequency band edge of $\varepsilon_{ll}''(\omega)$ being also nearly temperature independent. A calculation of the time dependence of the correlator $S_{ll}(t)$ for a harmonic chain [(1) with $V(X) = X^2$] using the analytic expression of $\varepsilon_{ll}''(\omega)$ (Ref. 8) also yields an oscillation (inset in Fig. 16). However, the corresponding frequency is $\omega_0^{\text{harm}} \approx 1.414 \approx \sqrt{2}$, which is the position of the *low*-frequency band edge of the high-frequency band of $\varepsilon_{ll}''(\omega)$. Thus the observed oscillation in $S_{ll}(t)$ for the $\Phi^4$ model has its origin in the nonlinearity of the model. It is unclear whether these oscillations might be connected with recently observed localized vibrations in nonlinear models, e.g., such as (1), with $V(X) = X^4$ (Ref. 38) (note that in such a case no kinks should be present) or not. This remains an interesting question.

## VI. SUMMARY

We studied the time dependence of a one-dimensional $\Phi^4$ lattice model with a NNI. For strong interaction we found a temperature region where two dynamic scaling laws for the displacement-displacement correlator $S_{ll}(t)$ appear. The analysis of these scaling laws brought out no applicability of mode-coupling equations for $S_{ll}(t)$. The scaling region is limited to $T > 0.15\sqrt{C}$. Thus the dynamic scaling cannot be attributed to the presence of a phase transition at $T_c = 0$. On the other hand, we find a drastic increase of the correlation length in the scaling

region. The imaginary part of the susceptibility $\varepsilon''(\omega)$ exhibits a low-frequency $\alpha'$ peak due to the presence of propagating kinks. At $T \approx 0.45\sqrt{C}$ the $\alpha'$ peak coalesces with the high-frequency part of $\varepsilon''(\omega)$. At this temperature $S_{ll}(t)$ exhibits a change of sign within the first period of its oscillation.

For weak interaction we found indications for one dynamic scaling law in $S_{ll}(t)$, which corresponds to the $\alpha'$ scaling in the strong-interaction case. The nonexistence of a second scaling law ($\beta'$ relaxation) again points to the nonapplicability of MCT.

The nonexistence of a structural relaxation such as, e.g., in undercooled liquids, is attributed to the presence of static on-site double-well potentials, which are mainly responsible for the relaxation of $S_{ll}(t)$ onto a plateau.

## APPENDIX A

In the following we will sketch the derivation to see that the pole of $M_q(z)$ in the Tserkovnikov representation (5)–(8) comes from the second line in (12). The equations of motion for a correlator, $((A|B))(z) = \text{LT}[\langle A(t)B \rangle]$, read

$$
\begin{aligned}
z((A|B)) &= (A|B) + i((\dot{A}|B)) \\
&= (A|B) - i((A|\dot{B})) ,
\end{aligned} \tag{A1}
$$

with $(A|B) = \langle AB \rangle$. Thus we obtain using $\lim_{t \to \infty} \langle A(t)A \rangle = L_{AA}$

$$
\lim_{z \to i0} ((\dot{A}|\dot{A})) = z(L_{AA} - (A|A)) , \tag{A2}
$$

$$
\lim_{z \to i0} ((\dot{A}|\ddot{A})) = -i(\dot{A}|\dot{A}) , \tag{A3}
$$

$$
\lim_{z \to i0} ((\ddot{A}|\dot{A})) = i(\dot{A}|\dot{A}) , \tag{A4}
$$

$$
\lim_{z \to i0} ((\dot{A}|A)) = -i(L_{AA} - (A|A)) , \tag{A5}
$$

$$
\lim_{z \to i0} ((A|\dot{A})) = i(L_{AA} - (A|A)) . \tag{A6}
$$

Using these properties we derive from (12)

$$
\lim_{z \to i0} M_q(z) = -\frac{L_q}{\chi_q^T(\chi_q^T - L_q/T)} . \tag{A7}
$$

Inserting (A7) into (4) one derives an identity 1=1.

Now let us analyze the Mori method for (1). For that we use the properties

$$
\langle A_{q_1} B_{q_2} \rangle = \langle A_{q_1} B_{-q_1} \rangle \delta_{q_1, -q_2}, \tag{A8}
$$

$$
\langle A|\hat{L}|B \rangle = -\frac{i}{\beta} \langle \{A^*, B\} \rangle \tag{A9}
$$

$$\{A, B\} = \sum_{n=1}^{N} \left[ \frac{\partial A}{\partial P_n} \frac{\partial B}{\partial X_n} - \frac{\partial A}{\partial X_n} \frac{\partial B}{\partial P_n} \right] \ . \tag{A10}$$

From

$$\hat{Q}\ddot{X}_q = \ddot{X}_q + X_q/\chi_q^T \ , \tag{A11}$$

we find with $n = 3$ for (14)

$$\hat{P}_{\text{MCT}}\ddot{X}_q \approx A\chi_q^{T-1} \sum_{q_2} \frac{X_{q_2}^2 X_q}{\langle |X_{q_2}|^2 \rangle} \ . \tag{A12}$$

We used the following approximation:

$$\langle X_{q_1}^* X_{q_2}^{*2} X_{q_1} X_{q_2}^2 \rangle \approx \langle |X_{q_1}|^2 \rangle \langle |X_{q_2}|^2 \rangle^2 \ . \tag{A13}$$

To calculate $\hat{P}_{\text{MCT}}X_q/\chi_q^T$ one has to treat averages $\langle X_q X_{q_1} X_{q_2} X_{q_3} \rangle$. If one decouples them using the approximation

$$\begin{aligned}
\langle X_q X_{q_1} X_{q_2} X_{q_3} \rangle \approx \ & \langle |X_q|^2 \rangle \langle |X_{q_2}|^2 \rangle \delta_{q,-q_1} \delta_{q_2,-q_3} \\
& + \langle |X_q|^2 \rangle \langle |X_{q_3}|^2 \rangle \delta_{q,-q_2} \delta_{q_1,-q_3} \\
& + \langle |X_q|^2 \rangle \langle |X_{q_1}|^2 \rangle \delta_{q,-q_3} \delta_{q_1,-q_2}
\end{aligned} \tag{A14}$$

it follows that $\hat{P}_{\text{MCT}}\hat{Q}\ddot{X}_q = 0$. This is not surprising, since the properties of (1) were not considered explicitly. Approximation (A14) becomes exact for, e.g., a harmonic chain, and there no relaxation kernel should appear. Thus the correct calculation of $V(q, q_1, q_2)$ in (15) remains an open question.

Substituting $\hat{Q}\hat{L}\hat{Q}$ in (9) and decoupling the time-dependent correlator

$$\langle X_{-q}(t) X_{-q_2}(t) X_{-q_3}(t) X_q X_{q_2} X_{q_3} \rangle$$

$$\approx \langle X_{-q}(t) X_q \rangle \langle X_{-q_2}(t) X_{q_2} \rangle \langle X_{-q_3}(t) X_{q_3} \rangle \ , \tag{A15}$$

we find (15).

## APPENDIX B

Here we want to briefly discuss the solutions of (4) and (13) near the phase transition $T_c = 0$ of (1).

With (13) one gets for $f_q = L_q/S_q(t = 0)$ (Ref. 4)

$$\frac{f_q}{1 - f_q} = 6T^2 \chi_q^T \int_{\text{1BZ}} dq_1 dq_2 f_{q_1} \chi_{q_1}^T f_{q_2} \chi_{q_2}^T f_{q-q_1-q_2} \chi_{q-q_1-q_2}^T \tag{B1}$$

Using the known critical behavior of the $d = 1$ Ising model[39] it follows that

$$\chi_q^{T-1} = e^{-C/T} + Cq \ . \tag{B2}$$

Inserting (B2) into (B1) and transforming $q \to Ce^{C/T}q$ one finds for $T \to 0$

$$\frac{f_q}{1 - f_q} = \frac{6T^2}{1 + q} e^{2C/T} C^{-2} \int_\infty dq_1 dq_2 \frac{f_{q_1} f_{q_2} f_{q-q_1-q_2}}{(1 + q_1)(1 + q_2)(1 + |q - q_1 - q_2|)}. \tag{B3}$$

Thus we obtain

$$f_q = 1 - A_q \frac{1}{T^2} e^{-2C/T} [1 + O(e^{-2C/T})] \ , \tag{B4}$$

with

$$\frac{1}{A_q} = \frac{6C^{-2}}{1 + q} \int_\infty dq_1 dq_2 (1 + q_1)^{-1} (1 + q_2)^{-1} (1 + |q - q_1 - q_2|)^{-1} \ . \tag{B5}$$

At $T = T_c = 0$, $f_q = 1$.

*Present address: Department of Physics, Boston University, 590 Commonwealth Avenue, Boston, Massachusetts 02215.

[1] A. D. Bruce and R. A. Cowley, *Structural Phase Transitions* (Taylor & Francis, London, 1981).

[2] K. A. Müller, in *Dynamical Critical Phenomena And Related Topics*, edited by C. P. Enz, Vol. 104 of Lecture Notes in Physics (Springer-Verlag, Berlin, 1979).

[3] V. L. Aksenov, M. Bobeth, N. M. Plakida, and J. Schreiber, J. Phys. C **20**, 375 (1987).

[4] W. Götze, in *Liquids, Freezing and the Glass Transition*, edited by J. P. Hansen, D. Levesque, and J. Zinn-Justin (North-Holland, Amsterdam, 1991).

[5] S. Flach, Z. Phys. B **82**, 419 (1991).

[6] S. Flach and E. Olbrich, Z. Phys. B **85**, 99 (1991).

[7] S. Flach, J. Siewert, R. Siems, and J. Schreiber, J. Phys. Condens. Matter **3**, 7061 (1991).

[8] S. Flach and J. Siewert, J. Phys. Condens. Matter **4**, L363 (1992).

[9] V. L. Aksenov, N. M. Plakida, and S. Stamenkovic, *Rasseanie Neitronov Segnetoelektrikami* (Energoatomisdat,

Moscow, 1984).

[10]P. W. Anderson, in *Physics of Dielectrics,* edited by G. I. Scanari (Acad. Nauk, Moscow, 1960).

[11]W. Cochran, Adv. Phys. **9**, 387 (1960).

[12]A. D. Bruce, T. Schneider, and E. Stoll, Phys. Rev. Lett. **43**, 1284 (1979).

[13]T. Schneider and E. Stoll, Ferroelectrics **24**, 67 (1980).

[14]S. Padlewski, A. K. Evans, C. Ayling, and V. Heine, J. Phys. Condens. Matter **4**, 4895 (1992).

[15]S. Aubry, J. Chem. Phys. **62**, 3217 (1975).

[16]S. Aubry, J. Chem. Phys. **64**, 3392 (1976).

[17]S. Aubry, Ferroelectrics **12**, 263 (1976).

[18]S. Aubry, Ferroelectrics **16**, 313 (1977).

[19]T. Schneider and E. Stoll, Phys. Rev. Lett. **31**, 1254 (1973).

[20]T. Schneider and E. Stoll, Phys. Rev. Lett. **35**, 296 (1975).

[21]T. Schneider and E. Stoll, Phys. Rev. B **17**, 1302 (1978).

[22]W. C. Kerr and A. R. Bishop, Phys. Rev. B **34**, 6295 (1986).

[23]B. Wiesen, K. H. Weyrich, and R. Siems, Phys. Rev. B **36**, 3175 (1987).

[24]S. Sarbach, Phys. Rev. B **15**, 2694 (1977).

[25]S. Flach, J. Siewert, R. Siems, and J. Schreiber, Ferroelectrics **124**, 173 (1991).

[26]W. Kob and R. Schilling, J. Phys. Condens. Matter **3**, 9195 (1991).

[27]E. Fick and G. Sauermann, *Quantenstatistik Dynamischer Prozesse* (Geest & Portig K.-G., Leipzig, 1985), Vol. IIa.

[28]Yu. A. Tserkovnikov, Theor. Mat. Fiz. **49**, 219 (1981).

[29]Yu. A. Tserkovnikov, Theor. Mat. Fiz. **50**, 53 (1982).

[30]S. Ma, *Modern Theory of Critical Phenomena* (Benjamin, London, 1976).

[31]S. Flach and E. Kornilov (unpublished).

[32]L. Verlet, Phys. Rev. **159**, 98 (1967).

[33]*Pocketbook of Mathematical Functions,* edited by M. Abramowitz and I. A. Stegun (Deutsch, Frankfurt, 1984).

[34]Y. Onodera, Prog. Theor. Phys. **44**, 1477 (1970).

[35]V. N. Prigodin, J. Phys. Condens. Matter **4**, 785 (1992).

[36]G. Li, W. M. Du, X. K. Chen, H. Z. Cummins, and N. J. Tao, Phys. Rev. A **45**, 3867 (1992).

[37]J. A. Krumhansl and J. R. Schrieffer, Phys. Rev. B **11**, 3535 (1975).

[38]S. Takeno and K. Hori, J. Phys. Soc. Jpn. **60**, 947 (1991).

[39]R. J. Baxter, *Exactly Solved Models in Statistical Mechanics* (Academic, London, 1982).